Energy-system optimization for hydrogen-based green steel production from medium-grade iron ore

Applied Energy 410 (2026) 127563

Contents lists available at ScienceDirect

Applied Energy

journal homepage: www.elsevier.com/locate/apenergy

Energy-system optimization for hydrogen-based green steel production from medium-grade iron ore

Marcel Stolte [a,b,*], Ali Bourig [c], Francesco Demetrio Minuto [a,b], Andrea Lanzini [a,b]

[a] Department of Energy, Politecnico Di Torino, Corso Duca Degli Abruzzi 24, 10129 Torino, Italy
[b] Energy Center Lab, Politecnico Di Torino, Via Paolo Borsellino 38/16, 10138 Torino, Italy
[c] EDF Power Solutions Australia, 210 George St, Sydney, NSW 2000, Australia

HIGHLIGHTS

- Optimization framework combines GA sizing with hourly MILP dispatch for green steel.
- Medium-grade ore analysed through hydrogen DRI with electric smelting.
- Hourly matching strongly influences hydrogen emissions and system cost.
- Threshold near 3 kg CO_2 $kg^{-1}H_2$ captures most abatement at lower marginal cost.

GRAPHICAL ABSTRACT

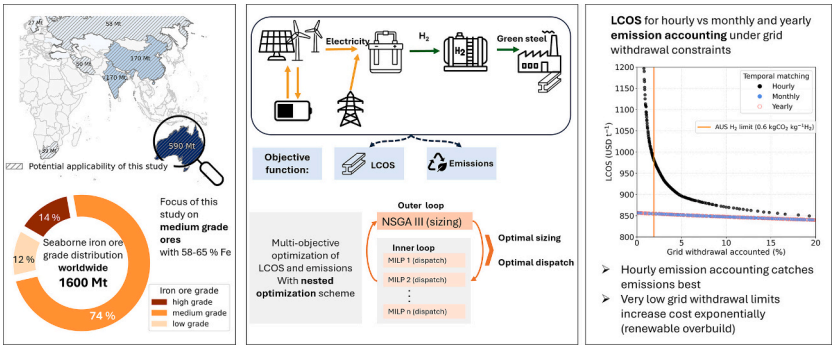

ARTICLE INFO

Keywords:
Green steel
Green hydrogen
Renewable energy
Multi-objective optimization

ABSTRACT

The steel industry accounts for 8% of global greenhouse gas emissions and is central to industrial decarbonization. Most green-steel assessments focus on hydrogen direct reduction with electric arc furnaces, which require high-grade ores. However, major iron ore producers, including Australia, the world's largest exporter, supply predominantly medium-grade ores that cannot be processed efficiently in this route. This study addresses this gap by assessing whether medium-grade ores can support competitive green-steel production. We develop an integrated optimization framework that links hydrogen supply, storage, and continuous steelmaking under variable renewable resources, applied to the hydrogen direct reduced iron-electric smelting furnace-basic oxygen furnace route tailored to medium-grade ores. The results show that an optimised mix of wind and solar power, supported by moderate grid supply, can lower production costs. The current cost gap of roughly 400 USD t^{-1} relative to conventional blast furnace steel can be closed through a combination of technology learning, carbon prices similar to the European Union Emissions Trading System, and targeted support that declines over time. Hourly temporal matching and limits on hydrogen-emission intensity have a strong influence on electrolyser utilisation, renewable overbuild, and the levelised cost of steel. A moderate emission threshold near 3 kg CO_2 $kg^{-1}H_2$, combined with hourly matching, captures most attainable abatement while avoiding the marked cost escalation associated with stricter limits. These findings clarify how ore quality, renewable-resource profiles, and

* Corresponding author at: Department of Energy, Politecnico Di Torino, Corso Duca Degli Abruzzi 24, 10129 Torino, Italy.
E-mail address: marcel.stolte@polito.it (M. Stolte).

https://doi.org/10.1016/j.apenergy.2026.127563
Received 4 December 2025; Received in revised form 11 February 2026; Accepted 13 February 2026
Available online 20 February 2026

hydrogen-system constraints interact to determine the feasibility of green steel production, and they offer guidance for regions planning large-scale hydrogen-based industrial systems.

1. Introduction

The iron and steel sector is a major source of industrial greenhouse gas emissions [1], making it one of the largest industrial contributors to climate change [2]. The dominant production route (BF-BOF), *blast furnace* (BF) combined with *basic oxygen furnace* (BOF), relies heavily on metallurgical coal and is inherently carbon-intensive. In contrast, the DRI-EAF route, *direct reduced iron* (DRI) route coupled with *electric arc furnaces* (EAF), offers a lower-emission alternative. However, the DRI-EAF route requires high-grade iron ore to operate efficiently (Fig. 1). Moreover, techno-economic constraints prevent EAFs from fully meeting primary steel demand [3].

Australia plays a pivotal role in the global steel value chain, supplying nearly 40% of the world's iron ore exports, predominantly from the Pilbara region [4]. However, this iron ore is typically of medium grade [5,6]. Medium and lower grade ores represent roughly 85% of global iron ore exports, and several major producers and consumers operate under similar resource constraints. This prevalence supports the broader relevance of studying hydrogen-based steelmaking routes adapted to medium-grade ores (Table 1 and Fig. 1c). In addition several of these producers possess high-quality wind and solar resources, implying that the policy and system-design insights developed here could be transferable to other jurisdictions pursuing green steel.

The global shift toward low-emissions steel creates both risks and opportunities for Australia. A transition led by high-grade DRI-EAF plants in major consuming regions could reduce demand for Australia's medium-grade ores [18]. At the same time, Australia's wind and solar resources provide favourable conditions for domestic production of green hydrogen and green steel [19–22]. Recent macroeconomic modelling also shows that relocating green steel production to renewable-rich regions may be more cost-effective than importing hydrogen, a trend described as "green relocation" and one with major

Table 1
Global iron ore producers, export shares, ore grades, and external validity of the Australian case.

Country	Share of global iron ore production on Fe Mt basis [7]	Share of global iron ore exports on Mt basis [8]	Typical iron ore grade	Relevance and replicability of this article
Australia	36.3%	55.9%	Medium grade [9]	Yes, as the major ore exporter
Brazil	17.5%	21.8%	High grade mostly [10]	Limited
China	10.6%	1.4%	Low grade; beneficiation necessary [11]	Yes, as a steel producer
India	10.6%	1.0%	Medium grade [12]	Yes, as a steel producer
Iran	3.7%	0.8%	Low to Medium grade [13]	Limited
Canada	2.0%	3.4%	Low grade upgraded to concentrates/ pellets [14]	Yes, as steel producer and ore exporter
South Africa	2.6%	3.7%	Medium grade [15]	Yes
USA	1.9%	0.7%	Low grade; beneficiation necessary [16]	Yes, as steel producer and ore exporter
Sweden	1.3%	1.5%	Medium grade; upgraded to high grade [17]	Limited

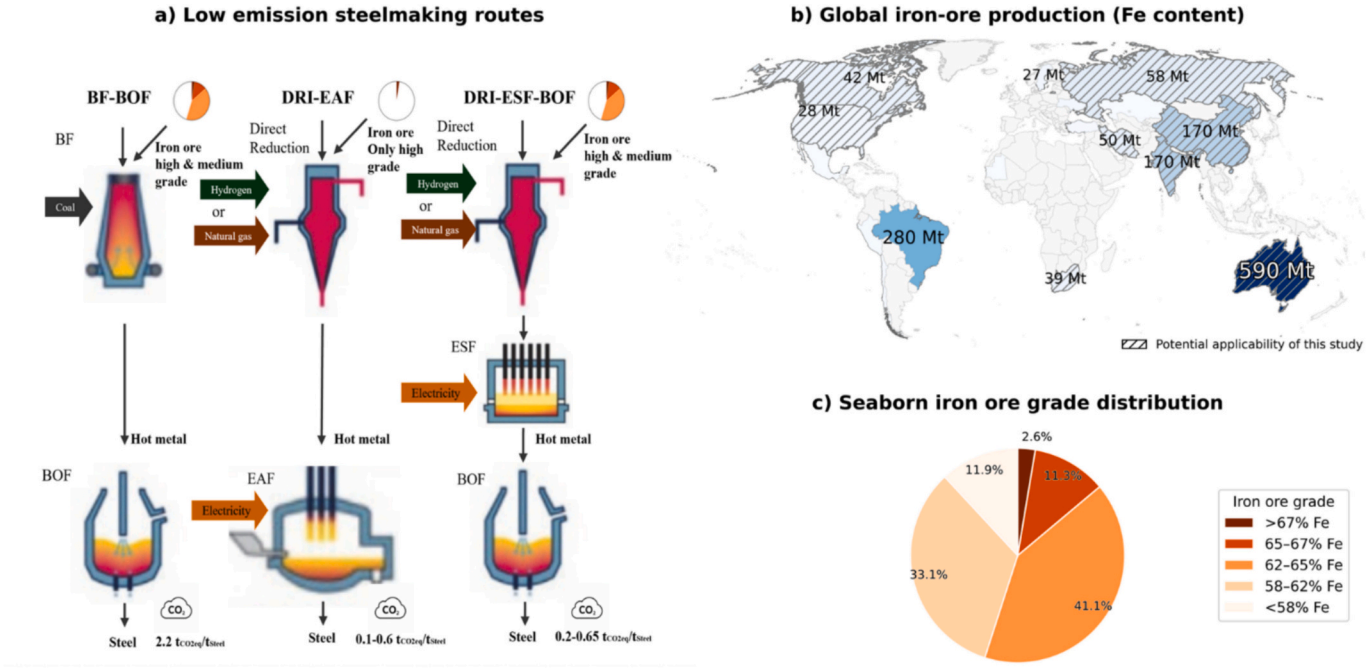

Fig. 1. a) Overview of primary steelmaking routes, visualizations adapted from [28,36]. The small pie charts on top visualize the compatible iron ore grades (after beneficiation). The resulting greenhouse gas emissions are visualized at the bottom, with the upper emission range in case of DRI-EAF and DRI-ESF-BOF to account for natural gas reduction and the lower values for green hydrogen DRI [26]. b) Global iron ore production by country. c) Seaborne iron ore export grouped by iron ore quality [16,26]. (For interpretation of the references to colour in this figure legend, the reader is referred to the web version of this article.)

implications for trade patterns and industrial competitiveness [23]. With highly favourable solar and wind resources Australia is well-positioned to shift from raw material exporter to low-emissions steel producer [24].

One promising technology is the *electric smelting furnace* (ESF), which can process medium-grade ores without the purity constraints of EAFs. In this route (DRI-ESF-BOF), hydrogen is used to reduce lower quality ores to DRI, which is then refined in an ESF and processed to steel in a BOF [25–28]. The reduction stage is fuel-flexible. DRI can be produced today with natural gas and later transition to hydrogen as supply decarbonises, including mixed-reductant operation, while the downstream ESF-BOF train remains unchanged. This staged pathway can lower near-term cost barriers but leaves a significant emissions residue that policy must explicitly bound. This retains the scale and metallurgical control of conventional steelmaking while eliminating coal and enabling integration with renewable electricity [29]. The route is currently being explored by multiple major industrial players [30]. Despite this growing industrial interest, the DRI-ESF-BOF route remains at an early stage, with no full-scale demonstration already in operation and persistent technical challenges ranging from refractory durability to process integration [21,26,31]. The academic literature remains limited, with most techno-economic analyses focusing on high-grade DRI-EAF systems [32,33], and only a few examining ESF-based reduction or ore-grade effects [27,28]. Recent work by Paymooni et al. [34] and Xue et al. [35] has analysed "ESF-based" systems with an emission abatement and process modelling focus, while treating energy supply as an exogenous parameter.

Despite the strategic importance of green hydrogen for decarbonizing hard-to-abate sectors such as steel and ammonia production, the global hydrogen industry faces significant challenges. A large number of announced projects have been delayed or cancelled due to economic and technical barriers [20,37]. Worldwide, many initiatives have been shelved due to high production costs, limited access to funding, and insufficient hydrogen demand. In the European Union, for example, green hydrogen deployment is falling significantly behind 2030 targets for both domestic production and imports [38–40], and thereby undermining steel decarbonization targets.

A major obstacle to large-scale green steel production is the intermittency of renewable electricity, which complicates the continuous operation required by the DRI shaft furnace and the ESF. Variability in hydrogen supply can reduce system efficiency, accelerate electrolyser degradation, and increase storage requirements [41]. Without energy storage or firm renewable supply, green hydrogen production may instead rely on grid electricity, potentially undermining its emissions profile [15,16]. The evolution of hydrogen regulations adds further constraints, as standards for temporal correlation between renewable generation and hydrogen production can reduce electrolyser utilisation and increase system cost [42,43].

Hydrogen certification frameworks are being developed in the European Union, United States, China, and Australia. However, there is a significant misalignment regarding the requirements on temporal matching, additionality, and geographic correlation [44]. In Australia, the "Future Made in Australia" strategy and the Guarantee of Origin (GO) scheme have been introduced, establishing certification mechanisms for hydrogen. The scheme comprises two instruments: the Renewable Electricity Guarantee of Origin (REGO), which provides time-stamped tracking of renewable electricity inputs, and the Product Guarantee of Origin (PGO), which certifies emissions intensity of commodities like hydrogen and green steel. Together, they enable transparent differentiation of renewable hydrogen. Under the current GO design, temporal correlation is satisfied on an annual basis. REGOs are time-stamped but no start date is specified for mandatory hourly correlation or full additionality requirements [45,46].

In the United States, the *Inflation Reduction Act* offers a tax credit of up to USD 3 per kilogram of low-carbon hydrogen under Section 45 V, conditional on lifecycle emissions thresholds.

Temporal matching is annual until 2029 and hourly from 1 January 2030 and coupled to additionality and deliverability provisions [47,48].

The European Union, through the *Renewable Energy Directive (RED II)* and delegated acts, mandates that hydrogen, classified as *Renewable Fuel of Non-Biological Origin* (RFNBO), achieve at least a 70% emissions reduction relative to conventional hydrogen. The delegated acts specify monthly temporal correlation until 31 December 2029 and hourly correlation from 1 January 2030. Additionality requirement and geographic correlation also apply [49,50].

In China, the Medium- and Long-Term Plan for Hydrogen Energy Industry Development (2021–2035) and the 15th Five-Year Plan support green hydrogen and green steelmaking [51]. As of the end of 2024, China is not only on track to exceed its 2025 green hydrogen deployment target but also leads globally in hydrogen production and consumption, while accounting for more than half of installed electrolyser capacity and around 90% of manufacturing output [38]. To provide common standards and avoid high emissions, the China Hydrogen Alliance established an initial 'clean hydrogen' threshold of 4.9 kg CO_2 kg^{-1} H_2 [51]. However, the regulatory framework is evolving rapidly, and rules regarding temporal matching remain under development. In 2025 the National Energy Administration launched a hydrogen pilot programme covering priority areas across the value chain, from large-scale electrolysers (>100 MW) to transportation and storage and low-carbon transformation of energy-intensive industries [52]. Meanwhile, rising demand from electric vehicle manufacturers and other industrial users continues to drive interest in low-emissions steel [53].

Despite the urgency of these challenges, a critical gap remains in the literature. Most techno-economic assessments prioritize the DRI-EAF route, which inherently assumes the availability of high-grade ores and often models hydrogen supply under simplified annual constraints. Existing ESF- and OSBF-focused studies and reviews largely concentrate on metallurgical feasibility, process integration, or static cost comparisons, treating energy supply, renewable variability, and hydrogen availability as exogenous inputs. While recent studies have begun to address the cost implications of green hydrogen certification, they rarely integrate the specific thermodynamic and economic realities of processing medium-grade ores via the ESF route, within a high-resolution energy-system framework. Consequently, the combined non-linear impact of ore quality, renewable variability, and strict hourly temporal matching on system design remains unknown. Understanding this intersection is vital for major producers like Australia, where the feasibility of green steel hinges on reconciling abundant medium-grade reserves with increasingly stringent international compliance standards.

The study investigates the following research question:

- How do operational constraints on hydrogen production, such as hourly matching and emission-intensity limits, influence system design, cost, and emissions for hydrogen-based steelmaking using medium-grade ores?

We address the existing research gaps by:

- Designing an integrated DRI-ESF-BOF optimization framework. We introduce a nested optimization structure for sizing and dispatch that simultaneously captures non-linear economies of scale and strict hourly dispatch constraints. This overcomes the limitations of standard linear models, enabling precise trade-off analysis between capital intensity and operational flexibility.
- Establishing a novel quantitative link between temporal matching stringency and steel production costs. By mapping the non-linear escalation of abatement costs against hourly grid-withdrawal limits, we identify conditions where strict certification renders green steelmaking from medium-grade ore economically unviable.
- Defining the techno-economic architecture of the DRI-ESF-BOF pathway. By integrating the energetic constraints of continuous baseload operation with Australia's unique medium-grade ore

reserves and renewable profiles, we quantify the distinct storage and overbuild requirements necessary to compete with fossil-based incumbents. This provides a high-resolution blueprint for the world's largest iron ore exporter that is currently absent in the literature.

Cost sensitivities and future cost scenarios to 2050 are included to evaluate the role of technology learning. By analysing a route tailored to Australia's ore characteristics and renewable context, the study provides insights relevant to regions planning hydrogen-intensive industrial systems.

2. Methods

This study analyses the interactions between renewable supply, hydrogen production constraints, and the techno-economic feasibility of hydrogen-based steelmaking using medium-grade ore. A multi-objective optimization framework combines a genetic algorithm (GA) for system sizing with a mixed-integer linear programming (MILP) formulation for hourly dispatch. The framework captures the coupling between design and operation and quantifies the trade-offs between levelised cost of steel (LCOS) and the emission intensity of hydrogen production.

2.1. Optimization framework

Optimizing decarbonised steel production requires simultaneous capacity sizing of system components and assuring the optimal operation of the plant to produce steel at the lowest possible cost. This needs to consider volatility of the renewable energy production, use of the storage and also changing electricity prices.

The optimization problem contains the conflicting objectives to lower LCOS and reduce emissions by relying less on the electricity grid. Traditional MILP [54] based operational frameworks are very effective, however struggle with non-linearities, binary constraints and multi-objective optimisations [55]. To solve this challenge, we propose an optimization framework consisting of two loops, which can be seen in the Supplementary, Fig. 1 [56,57].

2.1.1. Outer loop: Capacity sizing (genetic algorithm)

The outer sizing loop consists of a genetic algorithm (GA) [58] searching over the vector x:

$$x = \{P_{PV}, P_{Wind}, P_{Electrolyser}, P_{BESS}, E_{BESS}, E_{H2-storage}\}. \quad (1)$$

where P denotes the power capacity of photovoltaic (PV) plant, wind, electrolysers and Li-ion battery energy storage system (BESS), and E denotes the corresponding energy capacities of the BESS and the hydrogen storage system. The GA explores the solution space to generate a Pareto front, minimizing two conflicting objectives: the LCOS and the specific carbon emission intensity of the produced steel [59]. Note that emission accounting is implemented as a post-dispatch fitness metric in the outer loop rather than a hard constraint in the inner MILP. This ensures that the dispatch remains economically optimal for a given system size, while the GA evolves the physical capacity of renewables and storage to structurally minimize grid reliance. We use the non-dominated Sorting Genetic Algorithm (NSGA) III implemented in the pymoo python library to do the outer loop optimization. The evolutionary process is configured with a population size of 100 and runs for 70 generations, totalling 7000 design evaluations. This budget was established via sensitivity analysis, ensuring Pareto front stabilization and hypervolume convergence.

2.1.2. Inner loop: operational dispatch (MILP)

The inner optimization loop solves the hourly dispatch for each vector x proposed by the outer loop over one year, using a MILP algorithm. This formulation is necessary to capture the non-linear effect of battery replacement costs on LCOS, which varies significantly with the timing of reinvestment. We extrapolate the annual cycling rate to determine the specific replacement year and apply a piecewise linear discount factor using Special Ordered Sets of Type 2 (SOS2). Furthermore, binary constraints prevent simultaneous grid import and export, ensuring physical feasibility and accurate emissions accounting. Feasibility constraints include energy balances, storage state-of-charge and power limits and electrolyser load. We use the pyomo library in python for optimization and Gurobi 12.0.3 as the solver. More information on the optimization model is provided in the Supplementary.

The MILP evaluates each size set and optimises the LCOS for each given vector. The LCOS is calculated by dividing the total costs consisting of initial investment cost Inv, operation and maintenance costs $O\&M_j$, component replacement C_{repl_j} and grid electricity costs C_{grid_j} by the production of liquid steel P_{LS}.

$$LCOS = \frac{Inv + \sum_{j}^{m\_comp} \sum_{i=1}^{n=20} \frac{O\&M_j + C_{repl_j} + C_{grid_j}}{(1+r)^i}}{\sum_{i=1}^{n=20} \frac{P_{LS}}{(1+r)^i}} \quad (2)$$

In addition to LCOS, the emission intensity of the produced hydrogen ef_{H2} is calculated based on grid emission factor ef_{grid}, grid withdrawal P_{grid} and hydrogen production P_{H2}.

$$ef_{H2} = \frac{ef_{grid} \bullet \sum_{t=1}^{8760} P_{grid,t}}{\sum_{t=1}^{8760} P_{H2,t}} \quad (3)$$

After the optimization the LCOS of the solution and the emission factor is given back to the genetic algorithm to select a new set of sizes for the next generation. With this methodology a Pareto front [55] of optimal LCOS against emission intensity is created.

2.1.3. Steel production model

The model represents hydrogen-based reduction of medium-grade Pilbara ores followed by electric smelting and basic-oxygen refining. Due to the higher gangue content of medium-grade ore, the DRI-ESF-BOF route is used, consistent with previous techno-economic studies [28,31,35,60]. Hydrogen consumption in the shaft furnace is set to 59.4 kg H_2 t^{-1} DRI, to represent a process with iron ore of medium grade. This incorporates a moderate excess with respect to the stoichiometric quantity needed [27,28]. A scrap share of 0.13 t scrap t^{-1} liquid steel is included to reflect industry practice in primary routes [61].

Economic operation of a steel plant requires large scale. The case study fixes 2 Mtpa liquid steel production. The model converts this to constant hourly material and energy demands as a constraint for the MILP optimization. The nominal steel production capacity per hour $\dot{P}_{LS,nom}$ is based on the yearly steel production P_{LS} and the capacity factor cf of the plant and is expressed as:

$$\dot{P}_{LS,nom} = \frac{P_{LS}}{8760} * \frac{1}{cf} \quad (4)$$

The required quantities of iron ore can be calculated considering the necessary mass ratios of iron ore per DRI $r_{ore/DRI}$, DRI per hot metal $r_{DRI/HM}$, hot metal per liquid steel $r_{DRI/LS}$ and the scrap ratio r_{scrap}, as shown in Eq. (5).

$$r_{DRI/LS} = (1 - r_{scrap}) * r_{ore/DRI} * r_{DRI/HM} * r_{HM/LS} \quad (5)$$

The electricity demand in the smelting furnace $\dot{E}_{ESF}$ is modelled as a constant consumption with

$$\dot{E}_{ESF} = \dot{P}_{LS,nom} * \varepsilon_{ESF} \quad (6)$$

where ε_{ESF} is set at 0.5 MWh t^{-1} liquid steel, which accounts for smelting energy, slag formation, and associated thermal losses and lies within the range reported for smelting routes handling medium-grade feeds [35].

The steel plant operates continuously, considering a capacity factor of 90% to account for shutdowns and maintenance. In the energy model itself start-ups and short outages are outside the scope and implicitly absorbed by contingency factors in cost and availability. BOF oxygen, fluxes, and minor fuel utilities are accounted financially inside O&M costs, but do not enter the electricity and hydrogen balances.

2.1.4. Energy supply model

Meeting the hydrogen demand of approximately 13 t h^{-1} and the ESF load requires a large diversified electricity portfolio consisting of dedicated utility-scale PV, onshore wind farms, and the grid. Hourly PV and wind production are simulated for 2024, while the grid covers residual demand subject to the operational constraints defined in Section 2.1.5 and analysed in Section 3.1. Hourly solar radiation data, ground temperature, windspeed and humidity for the Perth area were obtained from *Open-Meteo* [62]. The choice of location aligns with a planned ESF pilot plant [30]. This location combines existing infrastructure with proximity to Pilbara ore. Its renewable profile is also more globally representative than the Pilbara's extreme solar conditions. The PV plant uses monocrystalline modules with single-axis tracking and energy yields are calculated using the PV-lib python package [63]. Model choices like the DC/AC ratio, temperature model and fixed losses are reported in the Supplementary, Section 4.

Hourly wind speeds are taken from NASA Power reanalysis [64]. The conversion to hub-height speeds, air-density adjustment, the power-curve model and energy yield calculation are documented in the Supplementary, Section 5.

Grid electricity backfills deficits not met by PV, wind, and storage. We assume sufficient transmission capacity to ensure continuous steel plant operation, as connection studies are out of scope. Hourly wholesale prices are taken for the WEM/SWIS market in 2024 [65]. Developers may commonly hedge price risk using power purchase agreements. However, such data are not publicly available and still reflect underlying market value to a material degree [66]. Accordingly, the analysis uses observed wholesale prices with certificate and network adders as the most transparent price input. Further, we include network fees, to account for transmission, losses and grid infrastructure [67]. Because the required PV and wind capacities must likely be placed outside of the perimeter of the steel production site, the same network charges are applied to dedicated RES deliveries over the grid.

A utility scale Li-ion BESS enables load shifting and allows the electrolyser to operate with renewable energy even during periods of low renewable availability. The AC-AC round-trip efficiency is 85% [68], representing the mean lifetime efficiency to implicitly account for degradation, with SOC bounds 15–95% to preserve lifetime [69]. End-of-life is assumed at 8000 full equivalent cycles [70]. A cycle-counting degradation check is retained to trigger replacements in the cost stream, and the replacement time influences the levelised cost through discounting of the annual cashflows. To maintain operational characteristics over the project life and face the capacity fading problem, augmentation is required. We restrict the analysis to a single simulation year because ensuring the necessary temporal correlation between renewable generation and wholesale electricity prices is strictly required but unavailable for long horizons due to recent structural market changes. Furthermore, multi-decadal optimization presents a prohibitive computational burden. Consequently, capacity augmentation is represented inside the O&M costs [71].

Proton-exchange membrane (PEM) electrolysis is selected for its load-following capability, commercial maturity, and proven integration in renewable energy systems. High-temperature electrolysis is not included in this analysis as lifetime and cost projections remain highly uncertain. It is however acknowledged as a promising future option for cost reduction. The electrolyser is modelled with constant specific electricity consumption, justified by the plant's modular architecture. We select a representative mean lifetime value rather than a beginning-of-life specification to implicitly account for degradation. At low net load, modules are switched off to keep operating stacks near their efficient design range, rather than throttling all stacks. The model applies a deterministic stack replacement after 10 years [72].

To ensure continuous steel production, the system includes pressurised above-ground storage. Geological storage, like salt caverns in the Pilbara, or depleted oil/gas fields near Gingin and Dongara, can be lower-cost at large scale, but require site-specific geotechnical assessment and pressure admissibility studies [73–75]. To maintain transferability and limit site-specific uncertainty, geological options are excluded and we apply vessel storage cost assumptions for an operating range of 3–50 bar [56]. The outlet electrolyser pressure is assumed to be 30 bar, with a centrifugal compressor downstream to increase the storage pressure to 50 bar [56,76,77]. The energy demand for this compression is integrated into the plant's total electricity balance to ensure rigorous energy accounting. More detailed description of the storage constraints can be found in the Supplementary, Section 6.

2.1.5. Hydrogen emission accounting

Temporal correlation between renewable generation and hydrogen production is enforced at different resolutions. The main analysis uses hourly matching, and sensitivities explore monthly and annual matching. Certificate retirement follows Australia's large-scale generation certificate prices [78]. Emissions attribution applies the 2024 Western Australia (SWIS) emission factor of 570 g CO_2 kWh^{-1}, derived from the aggregation of Scope 2 and Scope 3 emissions [19,79]. In scenarios that include the Hydrogen Production Tax Incentive, the refundable tax offset is applied as a per-kilogram credit to the verified renewable hydrogen volume and subtracted from the hydrogen cost after the cost stream is calculated. The credit does not alter how the dispatch and optimal plant operation is computed [46].

2.2. Economic modelling

The input assumptions on equipment cost and other techno-economic parameters can be found in the Supplementary, Section 2.

There is a broad range of equipment cost observed across literature and different projections on future cost development. Moreover, cost estimates are often presented at different levels of detail and range from the Bare Erected Cost alone to more comprehensive figures that include hidden and indirect expenses up to the Total As-Spent Cost (TASC) level. To ensure consistency and improve the accuracy and practical relevance of our analysis, we harmonize all cost data to a common basis and use TASC as the reference metric [80]. Cost reductions are difficult to predict, and learning rates depend on the growth of cumulative global capacity. We model equipment cost C_n from a baseline C_0 using a one-factor learning curve, where the learning rate LR is defined as the percentage of cost reduction per capacity doubling. The new cumulative capacity is nominated n, while the baseline is represented by n_0. The cost Equation considering technology learning can be written as:

$$C_n = C_0 * (1 - LR)^{\log_2(n/n_0)} \tag{7}$$

Substantial shares of the LCOS are caused by investment costs related to electricity and hydrogen supply. We therefore apply Eq. (7) on the renewable energy production, battery storage and electrolysers at the TASC level and run a broad sensitivity analysis. The learning rates used are shown in Table 2.

3. Results

The results chapter is organized in three parts, analysing first the temporal matching of electricity production and consumption (Section 3.1). Based on these findings we analyse the cost composition, impact of technology learning and competitiveness against alternative steelmaking routes (Section 3.2). The chapter concludes by examining hydrogen emission thresholds and the implications for policy design

Table 2
Cost reduction per capacity doublings.

	PV	Wind	BESS	PEM Electrolyser
Cost reduction per capacity doubling *LR*	21%[a] [81]	4%[a] [81]	11%[b] [82]	17%[c] [83,84]

Notes
[a] [81] IEA, World Energy Outlook 2024, 2024.
[b] [82] Schmidt O. et al., Nat. Energy, 2(8), 17110, 2017.
[c] [83,84] Bühler L., Möst D., Int. J. Hydrog. Energy, 89, 105–116, 2024; Weeda M., Detz R. J., TNO Report, 2022.

(Section 3.3).

3.1. Hydrogen temporal matching

We constructed a Pareto front, which represents the set of solutions where improving one objective worsens the other, to capture the trade-off between minimizing green steel production costs and maximizing emission reductions by limiting grid electricity withdrawal.

We repeated this optimization applying different temporal matching constraints for grid energy usage, from hourly up to yearly matching (Fig. 2a). The results show that hourly matching renders LCOS highly sensitive to grid withdrawal. When only few percent of the electricity supply can be taken from the grid the LCOS increases very steeply. Moving to monthly or yearly accounting the LCOS curve flattens and is much less sensitive to low grid withdrawal. The reason for the flatter curve for monthly and yearly accounting is that the lower granularity does not catch the actual grid interactions. We use the 1.9% grid withdrawal point as the reference case, representing the maximum grid share that satisfies the Australian hydrogen emission threshold of 0.6 kg CO_2 kg^{-1} H_2 (Fig. 2a and b). Comparing the accounted grid emissions withdrawal with the actual grid exchanges on an hourly basis, it emerges that the temporal matching requirement has a large influence on how much of the emissions are actually accounted. While for hourly accounting the real and accounted grid exchanges both amount to 1.9%, moving to monthly and yearly accounting, the actual grid exchanges increase to 18.2% and 18.3% respectively. This means that monthly or annual accounting catches less than 11% of actual grid withdrawal. For this reason we base the following analyses on hourly accounting.

3.2. Analysis on cost and technology competitiveness

Reducing grid electricity withdrawal raises steel production costs (Fig. 3), primarily due to the need for overbuilt renewable infrastructure to ensure year-round hydrogen and electricity supply for the DRI and steel plant.

The biggest sensitivity toward grid withdrawals can be observed at external electricity contributions of less than 5%, where it becomes increasingly expensive to cover the most unfavourable and prolonged shortage periods. Even small amounts of grid withdrawal at these stages can substantially reduce the need for oversizing renewable generation and storage. For the lowest grid withdrawal and based exclusively on self-produced renewable electricity LCOS above 1500 USD t^{-1} are reached. These costs fall markedly as grid withdrawal rises, approaching a level of around 850 USD t^{-1}. Comparing these prices to fossil-based steelmaking routes, a significant cost gap occurs which is analysed in Fig. 5.

An analysis of the cost composition shows that capital costs for the

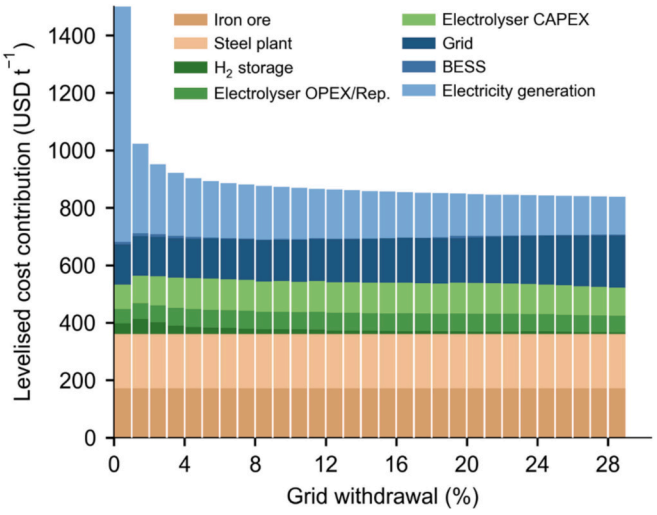

Fig. 3. Levelised cost of steel composition along the Pareto front, using today's cost assumption, excluding incentives. Costs are grouped into steelmaking, hydrogen supply and electricity supply.

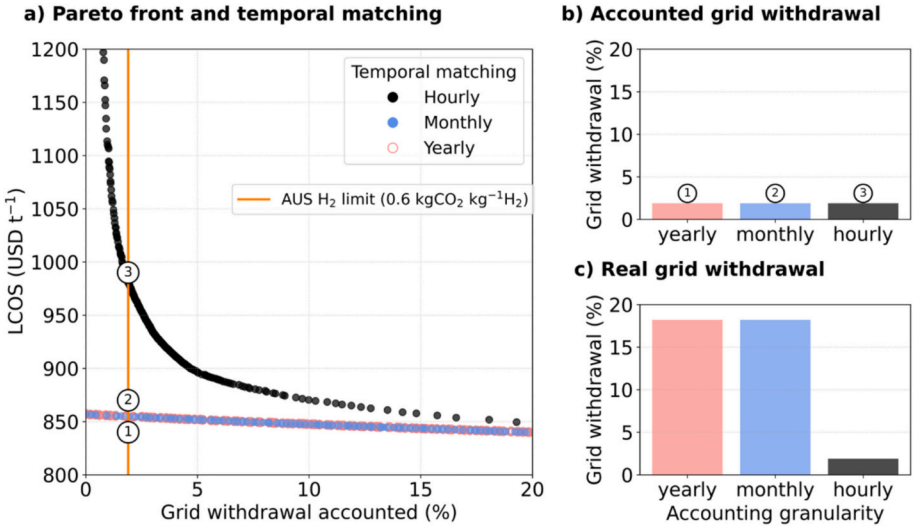

Fig. 2. a) Pareto front of grid-withdrawal and levelised cost of steel for different temporal matching granularity. b) Grid withdrawal accounted at the 0.6 kg H_2 kg^{-1} CO_2 limit to be in line with the Australian Hydrogen Production Tax Incentive threshold. Panel c) takes the simulations from b and analyses the actual grid withdrawal on an hourly basis and computes the average grid withdrawal of each accounting method.

DRI and steel plants, along with non-energy OPEX (brown areas), remain constant across grid withdrawal levels. This is caused by the modelling assumption to keep a continuous steel production all year round.

Costs directly associated with hydrogen production, including electrolyser investment cost, OPEX, replacements, and storage, are moderately sensitive to grid withdrawal levels. Especially the storage sizes increase significantly when looking at lower grid withdrawals. However, most sensitivity is caused by the electricity production for electrolysis and usage in the smelting furnace. While the optimal results for grid withdrawal below 1% show renewable generation capacities of more than 5 GW, it is reduced to 2 GW at the 28% grid withdrawal Pareto point. While BESS costs remain comparatively small, grid-related costs are substantial. These include not only the generation costs of external electricity but also transmission fees, applicable even to self-produced renewable electricity.

It emerges that the biggest cost factor is not the steel plant investment costs, causing less than 20% of LCOS. Therefore we focus further analysis on expenses for hydrogen and electricity supply.

To reach lower LCOS and cost competitiveness significant technology learning and cost reduction is necessary. Fig. 4 shows how cumulative capacity increases in capital-intensive components translate into lower steel costs, with component prices declining through deployment-driven learning effects, as described in Section 2.2. To maintain computational tractability within the nested optimization framework, we jointly evaluate capacity doublings for PV, wind, and BESS. This grouping reflects the strong economic correlation between these technologies, which are all driven by the broader global energy transition. The corresponding equipment cost can be found in the Supplementary, Section 2. Starting from today's cost assumptions (upper left cell), the model yields an LCOS of 877 USD t^{-1}, which decreases to 667 USD t^{-1} under the most ambitious capacity expansion scenario. To contextualize these capacity increases, the capacity increases according to IEA World Energy Outlook 2024 announced pledges scenario [81] are shown in Fig. 5 b).

While both technology learning in electrolysers and in electricity generation and storage lead to LCOS reduction, their effects are highly asymmetric. This asymmetry arises because global installed capacity of electrolysers is still at a very early stage, allowing for much larger multiplications of cumulative deployment than in the more mature components PV, Wind, and BESS. As a result, cumulative estimated learning in PEM electrolysers has roughly four times the leverage of cost reductions in the PV, Wind and BESS investments. For example, when the renewables supply chain is held at today's scale (bottom axis ×0), successive PEM capacity-increases drive the LCOS premium down by 19%. By contrast, the expected capacity increase until 2050 along the renewables supply chain without electrolyser learning, trims the LCOS by only 5%. Combining learning in both component groups yields the greatest absolute gain of 24%.

Benchmarking LCOS in Fig. 3 and Fig. 4 reveals that even in the most cost-optimised scenarios, green steel remains extremely costly. These results indicate that technology learning on the renewable energy and hydrogen side alone is unlikely to close the full cost gap against fossil based steel. Complementary levers such as carbon tax, or other targeted policy support are still required to achieve cost parity. To assess the policy interventions required for cost competitiveness, we modelled the cost gap relative to BF-BOF steel, being the most widely used primary steel production route.

Fig. 5 investigates the cost gap between hydrogen based steel and traditional steel production, which today amounts to almost 50%. For the 2025 case we selected the lowest cost of steel, which still respects the green hydrogen emission threshold of 0.6 kg CO_2 kg^{-1} H_2, leading to a grid withdrawal of 1.9% and an LCOS of 1006 USD t^{-1}. The total cost gap of this scenario amounts to more than 400 USD t^{-1}. The Australian head start tax credit for green hydrogen reduces this gap by 75 USD t^{-1}, covering 17% of the cost gap. The remaining 80% need to be filled by a carbon tax or carbon certificate schemes like the European Union Emissions Trading System (EU ETS), further incentives, or premiums for green products desired by customers. Even though Australia does not have a carbon tax in place, we took EU ETS level prices to visualize the effect.

Panel c traces the evolution of the cost gap from 2025 to 2050. In the 2050 scenario in Panel b, cost reductions of electricity and hydrogen production bring down the cost of green steel to 650 USD t^{-1}, which means a cost gap of approximately 20%. The two technologies are separated by a remaining cost gap of 136 USD t^{-1}. At this technological stage, no additional hydrogen incentives are applied. In this scenario a carbon price of 68 USD t^{-1} CO_2, lower than current prices of the EU ETS, would be enough to make the green steel cost competitive. Under higher carbon price trajectories, such as those projected in upper-range EU ETS estimates, green steel reaches competitiveness significantly earlier.

The long-term competitiveness of green steel depends not only on

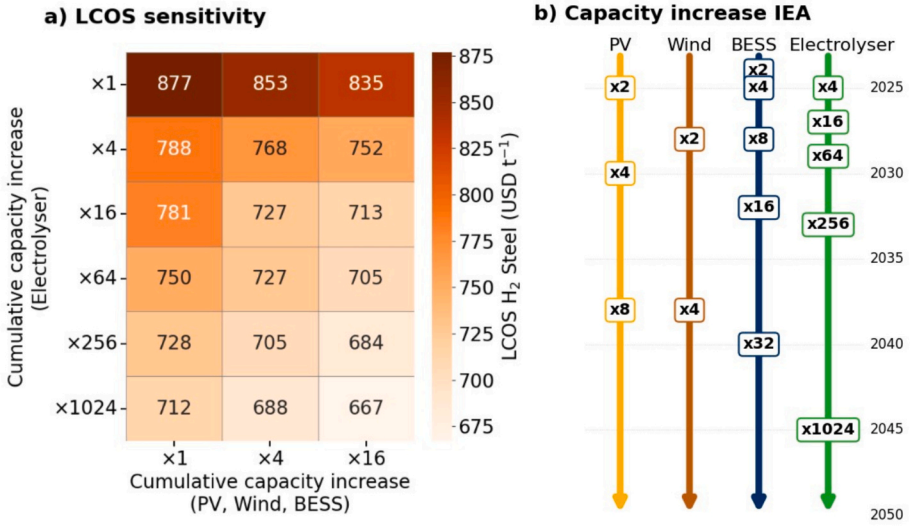

Fig. 4. a) Minimum levelised cost of steel looking at the effect of cumulative capacity increases, where PV, wind, and BESS are scaled simultaneously. Each cell contains the lowest-cost point on the Pareto front for the respective capacity increase scenario. The LCOS values reflect the techno-economic assumptions detailed in the Methodology chapter and exclude incentives. b) To reference when the capacity thresholds are achieved, we visualize the predicted capacity doublings by the IEA WEO 24 "announced pledges" scenario.

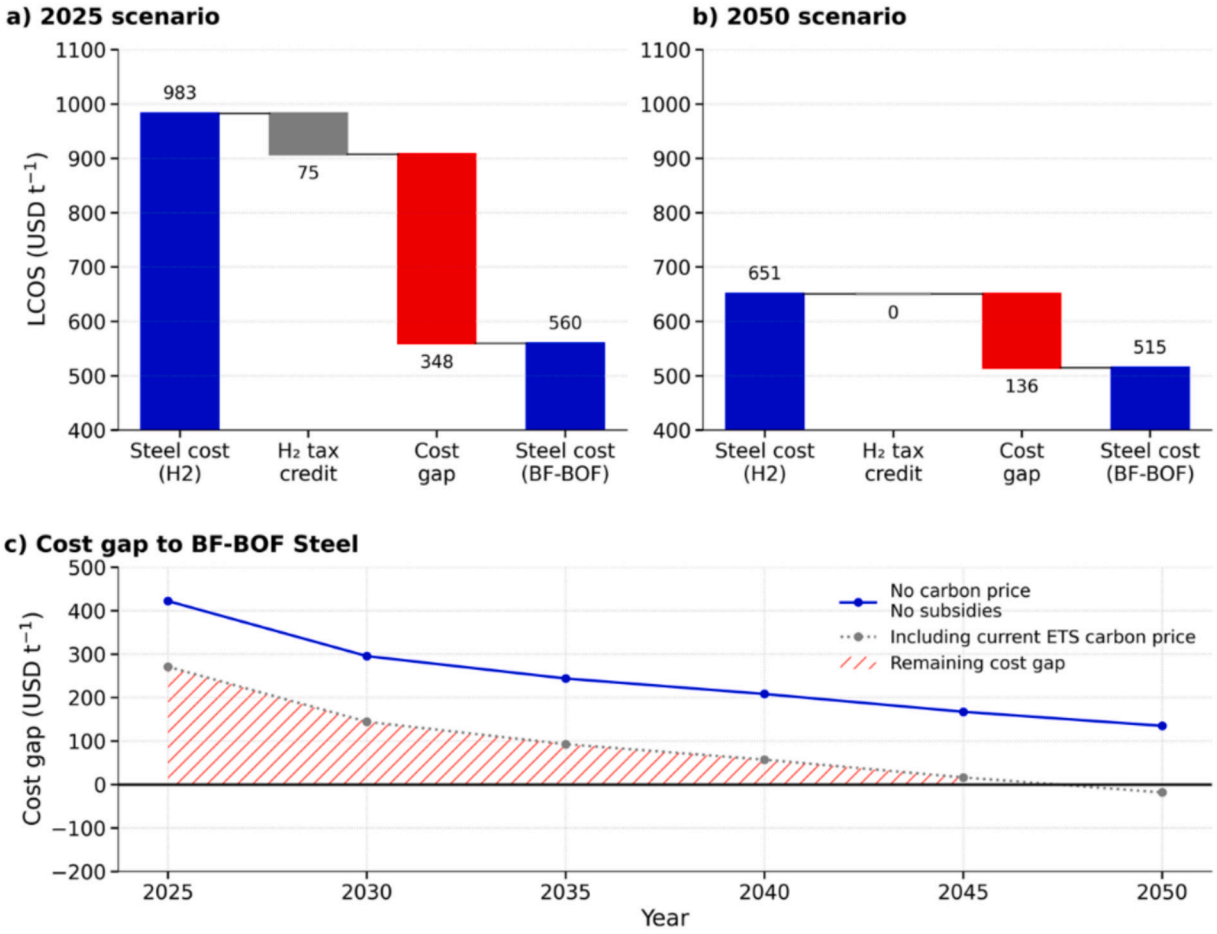

Fig. 5. Cost gap analysis between the investigated hydrogen DRI-ESF-BOF steel production and the BF-BOF based route. To visualize the potential effect of a carbon tax or emission trading system we used a hatched bar to represent a carbon certificate price of 85 USD $t^{-1}CO_2$ (current EU ETS price 2025). The area in red symbolizes a cost gap. Panel a) reflects current cost assumptions, whereas panel b) is based on IEA's 2050 mid-scenario capacity projections. Panel c) visualizes the development of the cost gap from 2025 to 2050. While the grey dotted curve shows the evolution of the cost gap including current EU ETS level carbon price [85], the red hatched area visualizes the remaining cost gap to BF-BOF steel. (For interpretation of the references to colour in this figure legend, the reader is referred to the web version of this article.)

absolute cost reductions but also on its position relative to alternative production routes under different carbon price trajectories. Fig. 6 maps

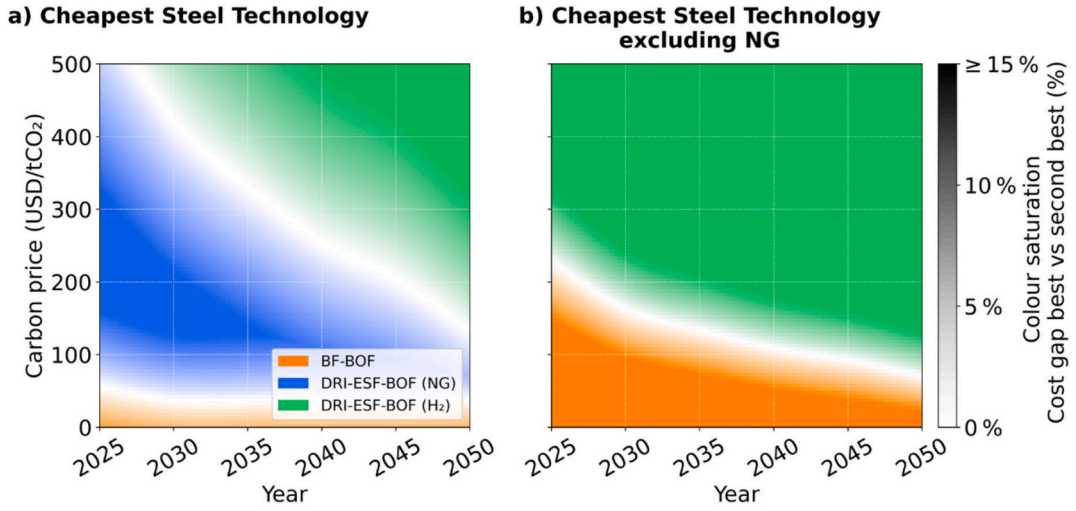

Fig. 6. Competitiveness map of the cheapest steelmaking technology. The analysis excludes hydrogen subsidies and is based on the IEA WEO 24 announced pledges scenarios to estimate technology learning for the respective years. Graph a) shows the comparison among three steelmaking routes, while b) excludes the natural gas based option. The saturation of the colours visualizes the dominance of the respective technology against the second best option. Lower saturation means that the LCOS are very close, while full saturation means a cost advantage of at least 15%.

this relative competitiveness, highlighting the conditions under which hydrogen-based DRI-ESF-BOF steelmaking could become the lowest-cost route compared to BF-BOF and natural gas-based steel production. Under current prices BF-BOF is the cheapest technology. Comparing this to natural gas-based steel production a carbon price of approximately 60 USD t^{-1} CO_2 is needed to make the natural gas-based solution competitive. Excluding natural gas among the options a carbon price of more than 200 USD t^{-1} CO_2 is required to make green steel close the cost gap.

The cost gap decreases over time, however, under the given assumptions even in 2050, if no carbon price or incentive scheme is in place, green steel will not be the cheapest option. However, due to the technology learning from electrolysis technology and renewables the needed carbon price is quickly approaching levels to what is projected in terms of future carbon prices. Natural gas appears to be a transitional solution, in several mid-range scenarios it is the most cost-effective option, although it leaves around 40% of emissions unabated.

3.3. *Effect of hydrogen emission limits on system design and marginal abatement cost*

Establishing credible carbon intensity thresholds for green hydrogen is critical to ensure climate integrity while maintaining economic feasibility. When thresholds are set too stringently, the cost of avoiding an additional tonne of CO_2 rises sharply, leading to excessive infrastructure requirements and prohibitive costs. If thresholds are too lenient, however, the emissions benefits relative to natural gas or grey hydrogen are undermined. Fig. 7 illustrates this trade-off by linking grid withdrawal levels to marginal abatement cost (MAC) under today's cost assumptions, providing a basis for defining thresholds that achieve substantial emission reductions at reasonable cost.

Fig. 7a shows the marginal abatement cost as a function of grid withdrawal percentage for the 2025 scenario, based on the Pareto front generated by the optimization model. The MAC represents the additional cost incurred to reduce carbon emissions of electricity withdrawal by one extra tonne compared to the neighbouring point on the curve. The definition of hydrogen emission limits is critical to LCOS, given that hydrogen production accounts for approximately 90% of the plant's total energy demand. Stricter limits on low-carbon hydrogen production consequently require low grid withdrawal percentages.

At low grid withdrawal levels, meaning scenarios relying mostly on dedicated renewable generation, MAC is very high and exceed 1000 USD per tonne CO_2 for grid-withdrawal below 2%. This is due to the fact that emissions are already strongly limited, and any further reduction requires disproportionately high investment and operational trade-offs. Conversely, at higher grid withdrawal levels, the marginal abatement costs decrease significantly. In scenarios with around 5–15% grid withdrawal, MAC values approach the range of current carbon removal costs, represented by the grey shaded area in the plot. These scenarios align more closely with realistic near-term decarbonization targets.

Different low-carbon hydrogen emission thresholds exist across a variety of countries and their practical impact is visually presented in Fig. 7a along the Pareto front. The associated subsidy levels are shown in Fig. 7b. Importantly, the absolute value of the subsidy cannot be considered in isolation and it must be interpreted alongside the strictness of the emission threshold and the temporal matching requirements discussed in Section 3.1. Australia enforces very stringent implicit grid withdrawal limits which, under the grid emission factor of 570 g CO_2 kWh^{-1}, permit only 1.9% grid usage. However, requirements in terms of additionality and temporal correlation are weak, since electricity from existing renewable plants and annual matching are still accepted [45,46]. The EU sets a less strict threshold of 3.38 kg CO_2 $kg^{-1}H_2$, corresponding to around 9% grid withdrawal, but couples this with stricter temporal matching from 2030 and stricter additionality rules. In the United States, the Inflation Reduction Act defines a wide range of emission thresholds and incentives, being slightly less stringent than Australian levels, but enforce strict temporal matching from 2030.

4. Discussion

This study shows that the feasibility of green steel production from medium-grade ore is strongly influenced by the interaction between

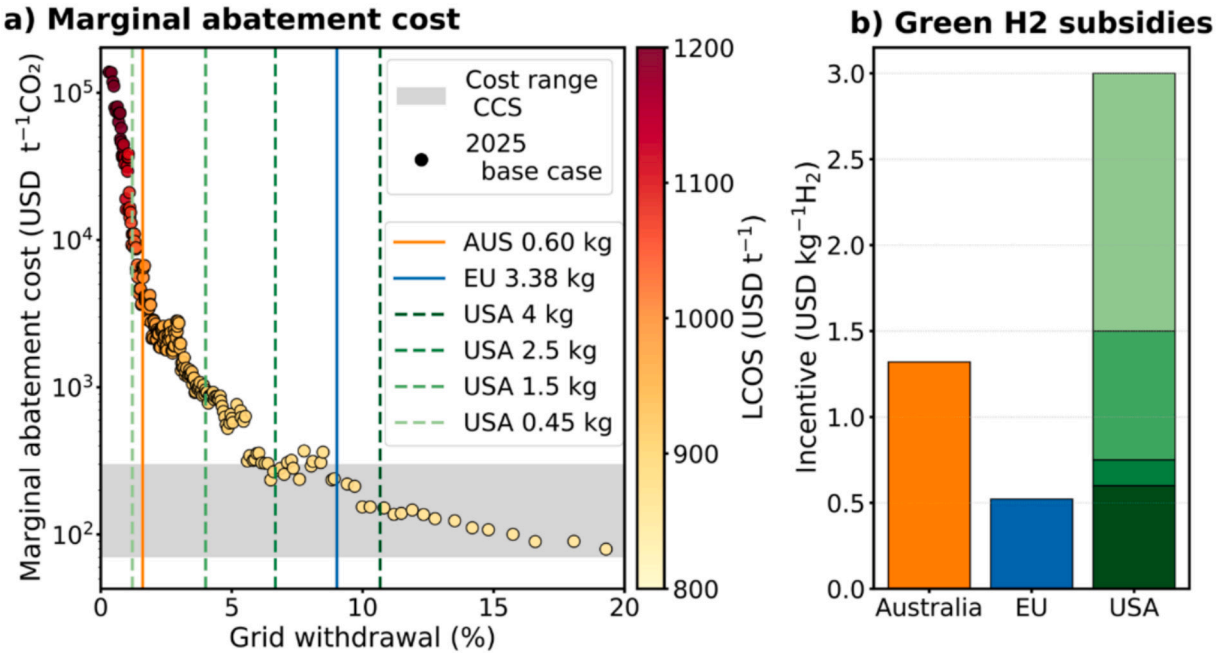

Fig. 7. a) Marginal abatement cost across different grid withdrawals, representing the Pareto front. The accounting of grid withdrawal is based on an hourly analysis for today's prices. The grey area shows current carbon capture and storage (CCS) cost range [86]. The noise in the curve is caused by the heuristic nature of the genetic algorithm to select the sizes. The vertical lines represents different greenhouse gas emission thresholds for green hydrogen in relation to hydrogen subsidies which are visualized in b). (For interpretation of the references to colour in this figure legend, the reader is referred to the web version of this article.)

renewable supply variability, hydrogen production constraints, and continuous plant operation. By integrating process-level data from emerging pilot studies into a 2 Mtpa system framework, this analysis explicitly links isolated technical insights to the requirements of large-scale industrial operation.

4.1. System-level implications for green steel deployment

Australia aims to retain leadership in iron ore exports while capturing more value in low-emissions products. National strategies and the emerging Guarantee of Origin framework seek to certify low-carbon hydrogen and enable trade in green commodities. Given uncertainties surrounding large-scale hydrogen exports, integrating hydrogen use within higher-value products such as DRI or green steel represents a pathway that aligns with existing logistics and reduces exposure to long-distance hydrogen transport. This pathway aligns industrial policy with climate objectives and reduces reliance on uncertain hydrogen transport value chains.

Achieving competitiveness in such products depends primarily on electricity price and carbon intensity. Even with technology learning, green steel from medium grade ores remains above BF-BOF costs, without either significant cost reductions in power and electrolysis or explicit carbon pricing and targeted support. Carbon pricing trajectories strongly influence the competitiveness frontier between hydrogen-based and BF-BOF steelmaking. Simulations indicate that carbon prices at levels comparable to the EU Emissions Trading System would be enough to close the cost gap between hydrogen-based and conventional BF-BOF steel production before 2045. Nevertheless, near-term parity remains challenging without additional support. When accounting for both projected technology learning and EU ETS-level carbon pricing, we calculated a remaining cost gap of 125 USD t^{-1} liquid steel in 2030, which reduces to 38 USD t^{-1} in 2040. This remaining gap would need to be covered by further subsidies or accelerated technology cost reductions to achieve full competitiveness.

Due to the currently high cost, natural gas-based DRI represents a plausible transitional route and was found to be the most cost-efficient configuration across a broad range of carbon prices and technology cost assumptions. Comparing these operating concepts exposes a clear trade-off. While the NG-based route offers lower capital intensity and less exposure to renewable intermittency, it lacks the structural flexibility to adapt to the shifting competitiveness frontier and carbon pricing. While reducing iron ore with natural gas can deliver moderate emissions reductions relative to BF-BOF and utilize existing assets, they still leave 30–40% of process emissions unabated. Additionally, reliance on natural gas introduces exposure to fossil fuel price volatility and geopolitical supply risks. Crucially, from a policy perspective, widespread adoption of NG-based steel risks locking in carbon-intensive infrastructure and delaying investment in truly zero-emission alternatives. Natural gas-based pathways require careful consideration, as widespread adoption could prolong emissions and delay investment in zero-carbon routes.

Hourly temporal matching strongly reduced realised system emissions by aligning hydrogen production with renewable availability. Annual matching understates real emissions by allowing electrolysers to treat the grid as free storage, shifting stress and emissions to the power system and obscuring the value of storage and curtailment. Hourly accounting corrects this by aligning hydrogen production with periods of renewable availability and by revealing when grid power is scarce or carbon-intensive. While in the EU and USA hourly accounting will start from 2030, Australia's GO scheme has introduced timestamped certificates but does not yet mandate hourly correlation, creating a gap with key export markets and with the physical realities of system operation.

Pairing hourly accounting with a moderate emission threshold avoids the prohibitive marginal abatement costs observed at very low grid withdrawals. Our results show MAC escalating beyond 1000 USD t^{-1} CO_2 when grid use falls below roughly 2%, while most of the abatement is already captured at modest withdrawals. If the threshold is too high, greenhouse gas abatement against fossil fuel based steel becomes negligible. If it is set too low, the already present cost barrier becomes prohibitive. The results indicate that a threshold around 3 kg CO_2 $kg^{-1}H_2$, combined with hourly matching, captures most achievable abatement without forcing disproportionate overbuild. This corresponds to about 9% grid withdrawal in Western Australia's current context and delivers credible emissions reduction without forcing excessive overbuild. This combination aligns with key export markets, preserves climate integrity, and supports early deployment. As renewable and storage costs fall with deployment, the cost-optimal design will shift toward higher shares of dedicated renewables and lower grid withdrawals, further reducing hydrogen-related emissions over time.

4.2. Limitations

This analysis is grounded in the Australian context, leveraging its abundant renewable resources, large land availability, and proximity to Asian markets. While Australia represents a relevant case as the leading iron ore exporter and an early adopter of hydrogen policy, repeating the analysis across jurisdictions would increase robustness. Regional differences in electricity prices, regulatory environments, or industrial infrastructure could affect both technical feasibility and economic outcomes. While absolute costs are specific to the Australian context, the identified non-linear trade-offs between emission thresholds and system design are universal. In regions with higher grid carbon intensity (e.g., India), admissible grid withdrawals would be lower, potentially increasing renewable overbuild. Conversely, regions with superior renewable resource quality or consistency might achieve higher electrolyser utilisation with lower storage requirements.

Several techno-economic assumptions introduce uncertainty. The cost and performance characteristics of Electric Smelting Furnaces are still largely unknown. Contrary to equipment related to energy supply we did not apply technology learning on the Steel plant investment costs. These parameters should be updated as more detailed technical data become available. Our model assumes conservative investment cost estimates and constant steel production, potentially overlooking flexibilities that could reduce energy costs. Additionally, we did not include hydropower plants or offshore wind farms, which could enhance the stability of electricity production around the year. These choices may underestimate potential options for energy firming and emissions mitigation. Furthermore, temporal resolution is limited to hourly timesteps over one year. Shorter intervals or multi-year simulations could reveal additional dynamics affecting storage needs, specifically regarding inter-annual resource variability and long-term degradation pathways, which are currently approximated via mean-lifetime parameters.

Future work should assess competitiveness across diverse regional contexts and extended planning horizons, incorporate dynamic steel plant operations, and explore hybrid or transitional technology routes.

5. Conclusions

This study evaluates the techno-economic feasibility of hydrogen-based steel production from medium-grade ores, focusing on the interaction between renewable variability, temporal correlation requirements, emission thresholds, and technology learning. Under current conditions, green steel from medium-grade ores exhibits an absolute cost gap of more than 400 USD t^{-1} of liquid steel relative to BF-BOF production. Projected cost reductions in electrolysers and renewable generation narrow this gap substantially by 2050. Carbon prices at levels comparable to the EU ETS eliminate the remaining cost gap before 2045. However, fostering short-term deployment would require additional support of about 125 USD t^{-1} in 2030, declining to around 38 USD t^{-1} by 2040. These results indicate that long-term cost-competitive green steel from medium-grade ores is challenging but attainable as energy-system costs fall and cumulative deployment increases.

High-granularity accounting, such as hourly matching, plays a central role in determining realised emissions because it reflects renewable variability and storage use, prevents the systematic underestimation of grid-related emissions that arises under annual averaging, and ensures that incentives drive genuine decarbonization. Pairing hourly accounting and additionality with a moderate hydrogen emission threshold balances climate integrity and feasibility. Our results indicate that thresholds that force very low grid withdrawals lead to prohibitive marginal abatement costs, whereas a threshold near 3 kg CO_2 $kg^{-1}H_2$ achieves most of the abatement at far lower cost and aligns producers with key export markets. Addressing technical bottlenecks such as refractory durability and optimizing dynamic plant operation remain priorities for future research to ensure the economic feasibility of these systems across diverse regional contexts.

Declaration of generative AI and AI-assisted technologies in the manuscript preparation process

During the preparation of this work the authors used ChatGPT in order to improve the language and readability of the manuscript. After using this tool/service, the authors reviewed and edited the content as needed and take full responsibility for the content of the published article.

CRediT authorship contribution statement

Marcel Stolte: Writing – review & editing, Writing – original draft, Visualization, Validation, Software, Methodology, Investigation, Data curation, Conceptualization. **Ali Bourig:** Supervision, Conceptualization. **Francesco Demetrio Minuto:** Writing – review & editing, Validation, Supervision, Project administration, Investigation, Conceptualization. **Andrea Lanzini:** Supervision, Resources, Project administration, Funding acquisition.

Declaration of competing interest

The authors declare the following financial interests/personal relationships which may be considered as potential competing interests: Co-author Ali Bourig is employed by EDF Power Solutions Australia. EDF Power Solutions Australia had no involvement in the conception, creation, analysis, editing, or decision to submit this article. The interpretations and conclusions expressed in this work are solely those of the authors and do not necessarily reflect the views of EDF Power Solutions Australia. If there are other authors, they declare that they have no known competing financial interests or personal relationships that could have appeared to influence the work reported in this paper.

Acknowledgements

M. Stolte carried out this study as part of the PNRR-NGEU project, which has received funding from the MUR – DM 117/2023, CUP: E14D23001950004. The scholarship is co-funded by Edison S.p.A.. This manuscript only reflects the authors' views and opinions, and neither the European Union nor the European Commission can be considered responsible for them.

Appendix A. Supplementary data

Supplementary data to this article can be found online at https://doi.org/10.1016/j.apenergy.2026.127563.

Data availability

Data will be made available on request.

References

[1] Iron and steel technology roadmap – analysis - IEA. Accessed: Apr 2025;09 [Online]. Available: https://www.iea.org/reports/iron-and-steel-technology-roadmap.
[2] OECD. 'OECD Steel Outlook 2025', *OECD Steel*. Outlook 2025. https://doi.org/10.1787/28b61a5e-en. May 2025.
[3] Solving iron ore quality issues for low-carbon steel. Accessed: Apr 2025;09:1–6 [Online]. Available: https://ieefa.org/resources/solving-iron-ore-quality-issues-low-carbon-steel.
[4] WA.gov.au | Western Australia's economy and international trade. Accessed: Apr 2025;09 [Online]. Available: https://www.wa.gov.au/government/publications/western-australias-economy-and-international-trade.
[5] Nicholas S, Basirat S. 'Solving iron ore quality issues for low-carbon steel', Institute for Energy Economics and Financial. Analysis 2022. Accessed: Aug. 28, 2025. [Online]. Available: https://ieefa.org/resources/solving-iron-ore-quality-issues-low-carbon-steel.
[6] Nicholas S, Basirat S. Iron ore quality a potential headwind to green steelmaking. Institut Energy Economics Financial Analysis 2022:1–38. Accessed: Aug. 28, 2025. [Online]. Available: https://ieefa.org/resources/iron-ore-quality-potential-headwind-green-steelmaking-technology-and-mining-options-are.
[7] Geological US. Mineral commodity summaries 2025. US Geol Surv 2025:2025. https://doi.org/10.3133/mcs2025.
[8] World mineral statistics data. MineralsUK Accessed: Oct 2025;10 [Online]. Available: https://www.bgs.ac.uk/mineralsuk/statistics/world-mineral-statistics/world-mineral-statistics-data-download/world-mineral-statistics-data/.
[9] Australia G. 'Iron', geoscience Australia. Accessed: Oct 2025;10 [Online]. Available: https://www.ga.gov.au/education/minerals-energy/australian-mineral-facts/iron.
[10] de Carvalho PSL, da Silva MM, Rocio MAR, Moszkowicz J. 'Minério de ferro', Mar. 2014, Accessed: Oct. 10 [Online]. Available: http://web.bndes.gov.br/bib/jspui/handle/1408/4802; 2025.
[11] USGS. Revision of global iron ore production data—Clarification of the reporting of iron ore production in China and application of a uniform comparison methodology (2000–2015). Accessed: Oct. 10. 2025 [Online]. Available: https://pubs.usgs.gov/publication/70238858.
[12] Rao ND, Chakraborty DP, Shukla V, Kumar N. Chapter 2 - Iron ore beneficiation: An overview. In: Rajendran S, Murty ChVGK, editors. Mineral processing. Elsevier; 2023. p. 55–77. https://doi.org/10.1016/B978-0-12-823149-4.00003-X.
[13] Majidi A, et al. Employing geochemistry and geochronology to unravel genesis and tectonic setting of iron oxide-apatite deposits of the Bafq-Saghand metallogenic belt, Central Iran. Int J Earth Sci 2021:1–38. https://doi.org/10.1007/s00531-020-01942-5.
[14] Dumont M. Iron Ore. 2008 [Online]. Available: https://natural-resources.canada.ca/sites/www.nrcan.gc.ca/files/mineralsmetals/pdf/mms-smm/busi-indu/cmy-amc/2008revu/pdf/iro-fer-eng.pdf.
[15] Gapara CS. A review of the deposition of iron-formation and genesis of the related iron ore deposits as a guide to exploration for Precambrian iron ore deposits in southern Africa. 1993. Accessed: Oct 10, 2025. [Online]. Available: https://vital.seals.ac.za/vital/access/manager/Repository/vital:4998?site_name=GlobalView&view=null&f0=sm_subject%3A%22Iron+ores+–+Geology+–+South+Africa%22&sort=sort_ss_title%2F.
[16] Mineral Commodity Summaries. US Geol Surv. 2024. 2024, 2024. doi:10.3133/mcs2024.
[17] Lundh J. A lithogeochemical study of northern Sweden and the Kiruna and Malmberget iron-apatite ore deposits. 2014. Accessed: Oct. 10, 2025. [Online]. Available: https://www.semanticscholar.org/paper/A-lithogeochemical-study-of-northern-Sweden-and-the-Lundh/13c9f181d1582066940e84d9854f4c5cfbde8d0a.
[18] Zhou T, Gosens J. 'China's green steel plans. Near-term policy challenges & Australia-China links in decarbonisation', Policy Brief. 2022 [Online]. Available: https://researchportalplus.anu.edu.au/en/publications/decarbonising-chinas-steel-industry.
[19] Australian government and Department of Climate Change, Energy, the Environment and Water. Australia's National Hydrogen Strategy - DCCEEW. 2024. Accessed: Oct. 27, 2024. [Online]. Available: https://www.dcceew.gov.au/energy/publications/australias-national-hydrogen-strategy.
[20] Odenweller A, Ueckerdt F. The green hydrogen ambition and implementation gap. Nat Energy 2025;10(1):110–23. https://doi.org/10.1038/s41560-024-01684-7.
[21] Rhee Y, O'Neill K, Al Ghafri SZS, May EF, Johns ML. Effect of location on green steel production using Australian resources. Int J Hydrog Energy 2024;90:827–41. https://doi.org/10.1016/j.ijhydene.2024.09.370.
[22] Burke PJ, et al. Contributing to regional decarbonization: Australia's potential to supply zero-carbon commodities to the Asia-Pacific. Energy 2022;248:123563. https://doi.org/10.1016/j.energy.2022.123563.
[23] Caiafa C, Kratena K, Arto I. Macroeconomic and environmental impacts of two decarbonization options for the Dutch steel industry: green relocation versus green hydrogen imports. Energy Policy 2025;206:114726. https://doi.org/10.1016/j.enpol.2025.114726.
[24] Australia Forges. A future made from green steel | Austrade international. Accessed: Apr. 09. 2025 [Online]. Available: https://international.austrade.gov.au/en/news-and-analysis/news/australia-forges-a-future-made-from-green-steel.
[25] Electric Melting. Furnaces for green steel transformation of integrated steel plants—requirements, challenges and solutions from a refractory perspective, RHI Magnesita. Accessed: Apr 15. 2025 [Online]. Available: https://www.rhimagnesita.com/the-bulletin-blog/electric-melting-furnaces-for-green-steel-

transformation-of-integrated-steel-plants-requirements-challenges-and-solutions-from-a-refractory-perspective/.
[26] Wimmer G, Fleischanderl A, Voraberger B. Green transition of the Iron and steel industry – impact on slags and by-products. ce/papers 2023;6(6):257–61. https://doi.org/10.1002/cepa.2954.
[27] Rahbari A, Shahabuddin M, Sabah S, Brooks G, Pye J. Production of green steel from low-grade ores: an end-to-end techno-economic assessment. Cell Rep Sustain 2025;2(1):100301. https://doi.org/10.1016/j.crsus.2024.100301.
[28] Sabah S, Shahabuddin M, Rahbari A, Brooks G, Pye J, Rhamdhani MA. Effect of gangue on CO2 emission for different decarbonisation pathways. Ironmak Steelmak 2024;51(4):356–68. https://doi.org/10.1177/03019233241242553.
[29] A Low-Carbon Emission. Flowsheet for BF-grade iron ore using advanced electric smelting furnace. Accessed: Apr. 15. 2025 [Online]. Available: https://www.hatch.com/About-Us/Publications/Technical-Papers/2023/05/A-low-carbon-emission-flowsheet-for-BF-grade-iron-ore-using-advanced-electric-smelting-furnace.
[30] BlueScope. BHP and Rio Tinto select WA for Australia's largest ironmaking electric smelting furnace pilot plant study. Accessed: Apr. 09. 2025 [Online]. Available: https://www.riotinto.com/en/news/releases/2024/bluescope-bhp-rio-tinto-wa-electric-smelting-furnace-study.
[31] Zhang Yale. The past, present and future of electric smelting furnaces. Steel Times Int 2023;47(3):24–6 [Online]. Available: https://www.scopus.com/record/display.uri?eid=2-s2.0-85188183502&origin=AuthorNamesList.
[32] Pimm AJ, Cockerill TT, Gale WF. Energy system requirements of fossil-free steelmaking using hydrogen direct reduction. J Clean Prod 2021;312:127665. https://doi.org/10.1016/j.jclepro.2021.127665.
[33] Li C, Zhang L, Wang Q, Zhou D. Towards low-carbon steel: system dynamics simulation of policies impact on green hydrogen steelmaking in China and the European Union. Energy Policy 2024;188:114073. https://doi.org/10.1016/j.enpol.2024.114073.
[34] Paymooni K, Garlick C, O'Dea D, Gadd A, Honeyands T. 'Emission abatement potential of DRI shaft furnace integrated with ESF-BOF process route', international congress on science and Technology of Ironmaking (ISCTI). 2025.
[35] Xue B, et al. Comparative analysis of process selection and carbon emissions assessment of innovative steelmaking routes. J Clean Prod 2024;451:142102. https://doi.org/10.1016/j.jclepro.2024.142102.
[36] Pfeiffer A, Rosner J, Voraberger B, Wimmer G. Smelter – Green Steelmaking Using Low-Grade DRI. 2024. p. 1935. doi:10.33313/388/202.
[37] Johnson N, Liebreich M, Kammen DM, Ekins P, McKenna R, Staffell I. Realistic roles for hydrogen in the future energy transition. Nat Rev Clean Technol 2025;1(5):351–71. https://doi.org/10.1038/s44359-025-00050-4.
[38] Global Hydrogen Review. Analysis, IEA. 2024. Accessed: Oct. 03, 2024. [Online]. Available: https://www.iea.org/reports/global-hydrogen-review-2024.
[39] Beyond the Hype: Hydrogen Gets Serious. S&P Global Commodity Insights. Accessed: Apr. 14. 2025 [Online]. Available: https://www.spglobal.com/commodity-insights/en/news-research/blog/energy-transition/102124-beyond-the-hype-hydrogen-gets-serious.
[40] Special Report. 11/2024: the EU'S industrial policy on renewable hydrogen, European Court of Auditors. Accessed: Apr 14. 2025 [Online]. Available: http://www.eca.europa.eu/en/publications/sr-2024-11.
[41] Nguyen E, Olivier P, Pera M-C, Pahon E, Roche R. Impacts of intermittency on low-temperature electrolysis technologies: a comprehensive review. Int J Hydrog Energy 2024;70:474–92. https://doi.org/10.1016/j.ijhydene.2024.05.217.
[42] Mingolla S, et al. Effects of emissions caps on the costs and feasibility of low-carbon hydrogen in the European ammonia industry. Nat Commun 2024;15(1):3753. https://doi.org/10.1038/s41467-024-48145-z.
[43] Vargas-Ferrer P, Jalil-Vega F, Pozo D, Sauma E. Complying with low-emission hydrogen standards in long-term integrated supply chains. Energy Policy 2025;198:114504. https://doi.org/10.1016/j.enpol.2025.114504.
[44] White LV, Fazeli R, Beck FJ, Baldwin KGH, Li C. Implications for cost-competitiveness of misalignment in hydrogen certification: a case study of exports from Australia to the EU. Energy Policy 2025;204:114661. https://doi.org/10.1016/j.enpol.2025.114661.
[45] Australian Government and Department of Climate Change. Energy, the Environment and Water, 'Guarantee of Origin Scheme - DCCEEW. Accessed: Apr. 14. 2025 [Online]. Available: https://www.dcceew.gov.au/energy/renewable/guarantee-of-origin-scheme.
[46] ParlInfo. Future Made in Australia (Production Tax Credits and Other Measures) Bill 2024. 2025. Accessed: Jul. 16, 2025. [Online]. Available: https://www.aph.gov.au/Parliamentary_Business/Bills_Legislation/Bills_Search_Results/Result?bId=r7297.
[47] US Government. Credit for production of clean hydrogen and energy credit', Federal Register Accessed: Apr 14. 2025 [Online]. Available: https://www.federalregister.gov/documents/2025/01/10/2024-31513/credit-for-production-of-clean-hydrogen-and-energy-credit.
[48] U.S. Department of the Treasury; Internal Revenue Service. Credit for production of clean hydrogen and energy credit90; 2025. p. 2224–332. Accessed: Jul. 31, 2025. [Online]. Available: https://www.federalregister.gov/documents/2025/01/10/2024-31513/credit-for-production-of-clean-hydrogen-and-energy-credit.
[49] EU, COMMISSION DELEGATED REGULATION (EU) *2023 /1184*. 2023. Accessed: Sep. 05, 2023. [Online]. Available: https://eur-lex.europa.eu/legal-content/EN/TXT/?toc=OJ%3AL%3A2023%3A157%3ATOC&uri=uriserv%3AOJ.L_.2023.157.01.0011.01.ENG.
[50] Commission Delegated Regulation (EU). 2023/*1185 of 10 February* 2023. 2023. Accessed: Nov. 09, 2023. [Online]. Available: http://data.europa.eu/eli/reg_del/2023/1185/oj/eng.
[51] China''s Hydrogen Sector. Balancing Growth and Challenges | Energy Partnership China-Germany. 2025. Accessed: Jan. 08, 2026. [Online]. Available: https://energypartnership.cn/publications-download-list/publications/chinas-hydrogen-sector-2025-balancing-growth-and-challenges/.
[52] Government of China, National Energy Administration. Notice of the general Office of the National Energy Administration on organizing and carrying out hydrogen energy pilot projects in the energy sector (National Energy Comprehensive Technology [2025] vol. No. 91). Apr. 07, 2025. Accessed: Aug. 27. 2025 [Online]. Available: https://www.nea.gov.cn/20250610/472b12c43f534aab9a95de81034dcd92/c.html..
[53] Shen J, Zhang Q, Tian S. Decarbonization pathways analysis and recommendations in the green steel supply chain of a typical steel end user-automotive industry. Appl Energy 2025;377:124711. https://doi.org/10.1016/j.apenergy.2024.124711.
[54] Kondili E, Pantelides CC, Sargent RWH. A general algorithm for short-term scheduling of batch operations—I. MILP formulation. Comput Chem Eng 1993;17(2):211–27. https://doi.org/10.1016/0098-1354(93)80015-F.
[55] Multiobjective Evolutionary Algorithms. A comparative case study and the strength pareto approach. Accessed: Sep. 08. 2025 [Online]. Available: https://xplorestaging.ieee.org/document/797969.
[56] Rozzi E, Grimaldi A, Minuto FD, Lanzini A. Model complexity and optimization trade-offs in the design and scheduling of hybrid hydrogen-battery systems. Energy Convers Manag 2025;344:120306. https://doi.org/10.1016/j.enconman.2025.120306.
[57] Yuan Y, et al. Multi-objective optimization and analysis of material and energy flows in a typical steel plant. Energy 2023;263:125874. https://doi.org/10.1016/j.energy.2022.125874.
[58] Deb K, Pratap A, Agarwal S, Meyarivan T. A fast and elitist multiobjective genetic algorithm: NSGA-II. IEEE Trans Evol Comput 2002;6(2):182–97. https://doi.org/10.1109/4235.996017.
[59] International Energy Agency. Towards hydrogen definitions based on their emissions intensity. OECD; 2023. https://doi.org/10.1787/44618fd1-en.
[60] Hamuyuni J, Tesfaye F, Vallo K, Haimi T, Pihlasalo J, Lindgren M. Fluxing options and slag operating window for Metso's sustainable DRI smelting furnace. JOM 2025;77(5):3446–56. https://doi.org/10.1007/s11837-025-07243-z.
[61] Bhaskar A, Abhishek R, Assadi M, Somehesaraei HN. Decarbonizing primary steel production : techno-economic assessment of a hydrogen based green steel production plant in Norway. J Clean Prod 2022;350:131339. https://doi.org/10.1016/j.jclepro.2022.131339.
[62] Zippenfenig P. Open-Meteo.com weather API. dec. 31. 2024. https://doi.org/10.5281/zenodo.14582479. Zenodo.
[63] Anderson KS, Hansen CW, Holmgren WF, Jensen AR, Mikofski MA, Driesse A. Pvlib python: 2023 project update. J Open Source Softw 2023;8(92):5994. https://doi.org/10.21105/joss.05994.
[64] NASA POWER. Data access viewer (DAV). Accessed: Aug. 21. 2025 [Online]. Available: https://power.larc.nasa.gov/data-access-viewer/.
[65] Market data. Clearing prices WEM market. Accessed: Aug. 21. 2025 [Online]. Available: https://www.aemo.com.au/energy-systems/electricity/wholesale-electricity-market-wem/data-wem/market-data-wa.
[66] Mittler C, Bucksteeg M, Staudt P. Review and morphological analysis of renewable power purchasing agreement types. Renew Sust Energ Rev 2025;211:115293. https://doi.org/10.1016/j.rser.2024.115293.
[67] Economic Regulation Authority, Western Australia. Annual Price lists for network charges - economic Regulation authority Western Australia. Accessed: Aug 21. 2025 [Online]. Available: https://www.erawa.com.au/electricity/electricity-access/western-power-network/annual-price-lists-for-network-charges.
[68] National Renewable Energy Laboratory. 'Electricity annual technology baseline (ATB) data 2022', National Renewable Energy. Laboratory 2022:1–65. Accessed: Jan. 23, 2024. [Online]. Available: https://atb.nrel.gov/electricity/2022/data.
[69] Stolte M, Minuto FD, Perol A, Bindi M, Lanzini A. Optimisation of green hydrogen production for hard-to-abate industries: an Italian case study considering national incentives. Int J Hydrog Energy 2025;141:1294–304. https://doi.org/10.1016/j.ijhydene.2025.03.008.
[70] Naumann M. 'Techno-economic evaluation of stationary battery energy storage systems with special consideration of aging', Technische Universität München. 2018 [Online]. Available: https://mediatum.ub.tum.de/doc/1434981/1434981.pdf.
[71] National Renewable Energy Laboratory. 'Annual technology baseline 2024', Tableau Software. Accessed: May 06. 2025 [Online]. Available: https://atb.nrel.gov/electricity/2024.
[72] Schmidt O, Gambhir A, Staffell I, Hawkes A, Nelson J, Few S. Future cost and performance of water electrolysis: an expert elicitation study. Int J Hydrog Energy 2017;42(52):30470–92. https://doi.org/10.1016/j.ijhydene.2017.10.045.
[73] Aftab A, Hassanpouryouzband A, Naderi H, Xie Q, Sarmadivaleh M. Quantifying onshore salt deposits and their potential for hydrogen energy storage in Australia. J Energy Storage 2023;65:107252. https://doi.org/10.1016/j.est.2023.107252.
[74] Dodangoda C, Ranjith PG, Haque A. Exploring hydrogen storage potential in depleted Western Australian hydrocarbon reservoirs: a petrophysical and petrographic analysis. Fuel 2024;358:129951. https://doi.org/10.1016/j.fuel.2023.129951.
[75] Für B-B, Klimaschutz W. BMWK veröffentlicht Weißbuch Wasserstoffspeicher. Accessed: May 05. 2025 [Online]. Available: https://www.bmwk.de/Redaktion/DE/Pressemitteilungen/2025/20250417-bmwk-veroeffentlicht-weissbuch-wasserstoffspeicher.html.
[76] Elberry AM, Thakur J, Santasalo-Aarnio A, Larmi M. Large-scale compressed hydrogen storage as part of renewable electricity storage systems. Int J Hydrog Energy 2021;46(29):15671–90. https://doi.org/10.1016/j.ijhydene.2021.02.080.

[77] Khan MA. 'The techno-economics of hydrogen compression', The Transition Accelerator. 2021. Accessed: May 05, 2025. [Online]. Available: https://transitionaccelerator.ca/reports/technical-brief-the-techno-economics-of-hydrogen-compression/.
[78] Australian Government. Large-scale generation certificates (LGCs) | clean energy regulator. Accessed: Aug. 29. 2025 [Online]. Available: https://cer.gov.au/markets/reports-and-data/quarterly-carbon-market-reports/quarterly-carbon-market-report-december-quarter-2024/large-scale-generation-certificates-lgcs?.
[79] Australian Government. Department of Climate Change, energy, the environment and water, 'Australian National Greenhouse Accounts Factors'. Australian government, Department of Climate Change, energy, the environment and water. 2024. Accessed: Jul 30, 2025. [Online]. Available: https://www.dcceew.gov.au/sites/default/files/documents/national-greenhouse-account-factors-2024.pdf.
[80] NETL. 'Cost estimation methodology for NETL assessments of power plant performance', National Energy Technology Laboratory. 2021 [Online]. Available: https://www.osti.gov/servlets/purl/1567736.
[81] World Energy. Outlook 2024 – Analysis. IEA; 2025. Accessed: Jul. 02. [Online]. Available: https://www.iea.org/reports/world-energy-outlook-2024.
[82] Schmidt O, Hawkes A, Gambhir A, Staffell I. The future cost of electrical energy storage based on experience rates. Nat Energy 2017;2(8):17110. https://doi.org/10.1038/nenergy.2017.110.
[83] Bühler L, Möst D. Derivation of one- and two-factor experience curves for electrolysis technologies. Int J Hydrog Energy 2024;89:105–16. https://doi.org/10.1016/j.ijhydene.2024.09.243.
[84] Weeda M, Detz RJ. Projections of electrolyzer investment cost reduction through learning curve analysis, TNO; e ministry of economic affairs and climate policy, Netherlands. 2022 [Online]. Available: https://energy.nl/wp-content/uploads/tno-2022-p10111_detzweeda_projections-of-electrolyzer-investment-cost-reduction-through-learning-curve-analysis.pdf.
[85] C. Günther, M. Pahle, K. Govorukha, S. Osorio, and T. Fotiou, 'Carbon prices on the rise? Shedding light on the emerging second EU emissions trading system (EU ETS 2)', *Clim Pol*, vol. 0, no. 0, pp. 1–12, doi:https://doi.org/10.1080/14693062.2025.2485196.
[86] CCUS. In clean energy transitions – analysis. IEA; 2025. Accessed: Sep 16. [Online]. Available: https://www.iea.org/reports/ccus-in-clean-energy-transitions.